Surface Winds and Enthalpy Fluxes During Tropical Cyclone Formation From Easterly Waves: A CYGNSS view

Anantha Aiyyer[1] and Carl Schreck[2]

[1]North Carolina State University
[2]Cooperative Institute for Satellite Earth System Studies (CISESS), North Carolina State University, Asheville

November 23, 2022

Abstract

We examined the Cyclone Global Navigation Satellite System (CYGNSS) retrievals of surface winds and enthalpy fluxes in African easterly waves that led to the formation of 31 Atlantic tropical cyclones from 2018–2021. Lag composites show a cyclonic proto-vortex as early as 3 days prior to tropical cyclogenesis. The distribution of enthalpy fluxes within the proto-vortex does not vary substantially prior to cyclogenesis, but subsequently, there is an increase in the upper extreme values. A negative radial gradient of enthalpy fluxes becomes apparent as early as 2 days before cyclogenesis. These results—based on a novel data blending satellite retrievals and global reanalysis—are consistent with recent studies that have found that tropical cyclone spin-up is associated with a shift of peak convection towards the vortex-core and a radially inward increase of enthalpy fluxes. They provide additional evidence for the importance of surface enthalpy fluxes and their radial structure for tropical cyclogenesis.

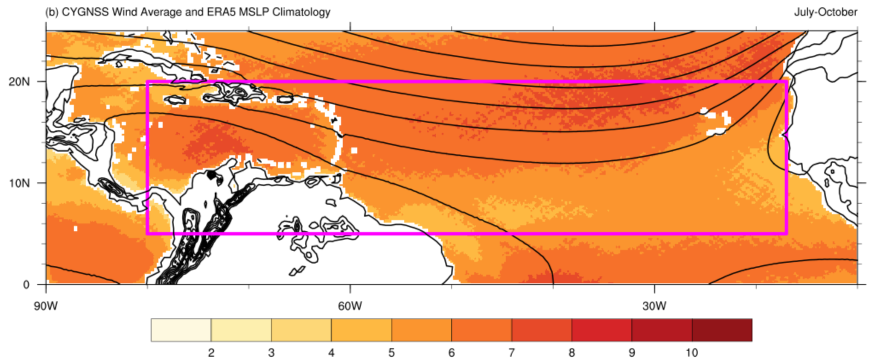
(b) CYGNSS Wind Average and ERA5 MSLP Climatology
July-October
20N
10N
0
90W
60W
30W
2
3
4
5
6
7
8
9
10

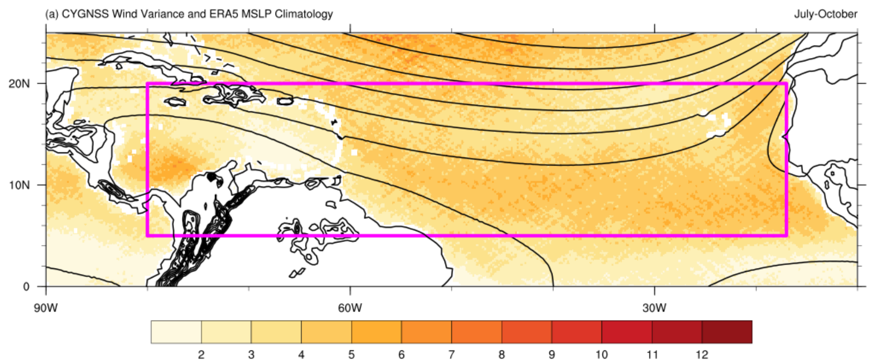
(a) CYGNSS Wind Variance and ERA5 MSLP Climatology
July-October
20N
10N
0
90W
60W
30W
2
3
4
5
6
7
8
9
10
11
12

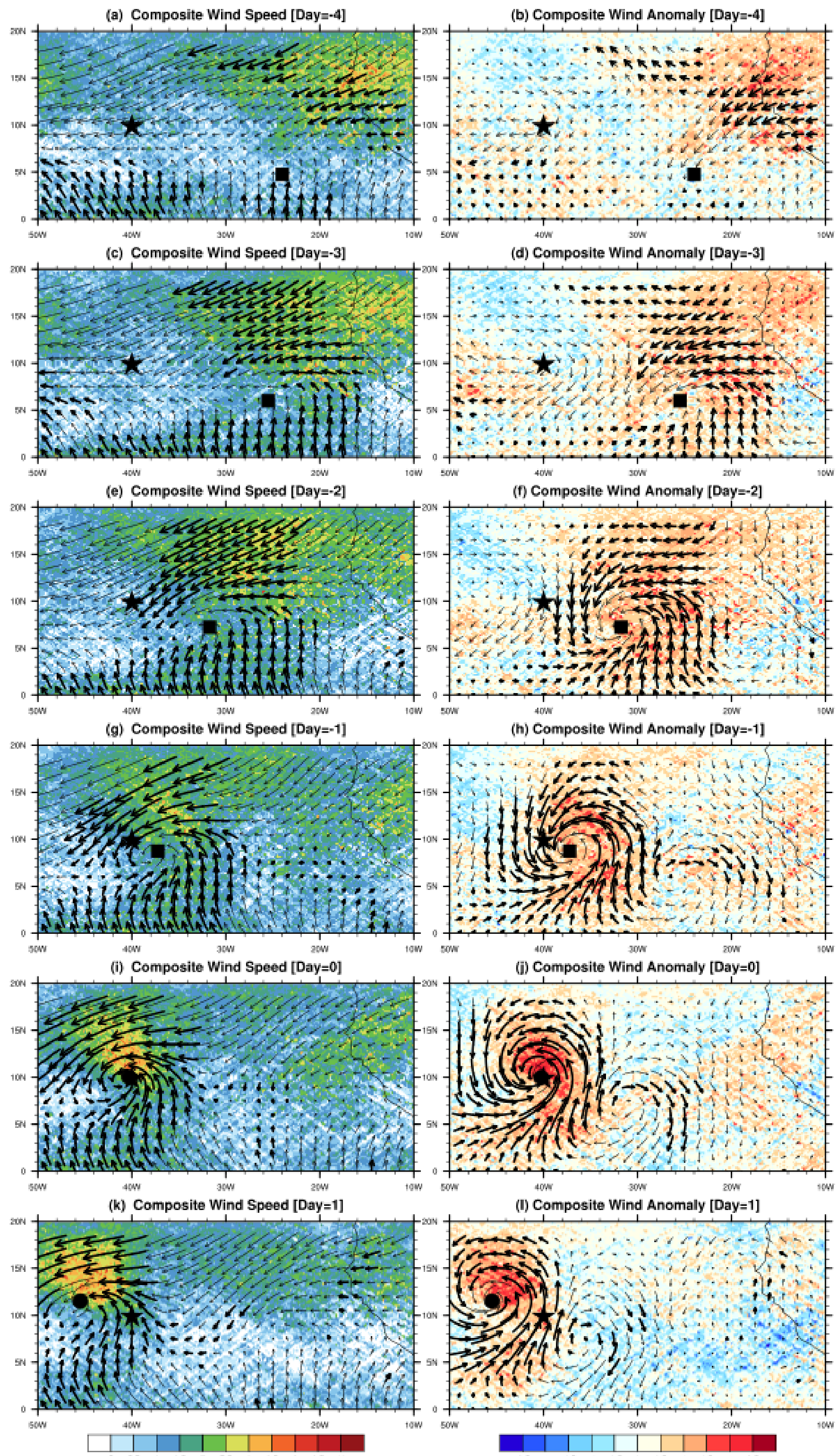
(a) Composite Wind Speed [Day=-4]
(b) Composite Wind Anomaly [Day=-4]
(c) Composite Wind Speed [Day=-3]
(d) Composite Wind Anomaly [Day=-3]
(e) Composite Wind Speed [Day=-2]
(f) Composite Wind Anomaly [Day=-2]
(g) Composite Wind Speed [Day=-1]
(h) Composite Wind Anomaly [Day=-1]
(i) Composite Wind Speed [Day=0]
(j) Composite Wind Anomaly [Day=0]
(k) Composite Wind Speed [Day=1]
(l) Composite Wind Anomaly [Day=1]
20N
15N
10N
5N
0
50W
40W
30W
20W
10W
5 5.5 6 6.5 7 7.5 8 8.5 9 9.5 10
-2.5 -2 -1.5 -1 -0.5 0 0.5 1 1.5 2 2.5

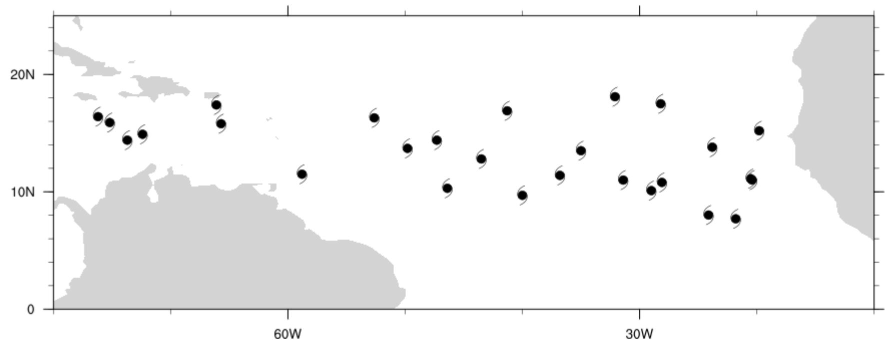
20N
10N
0
60W
30W

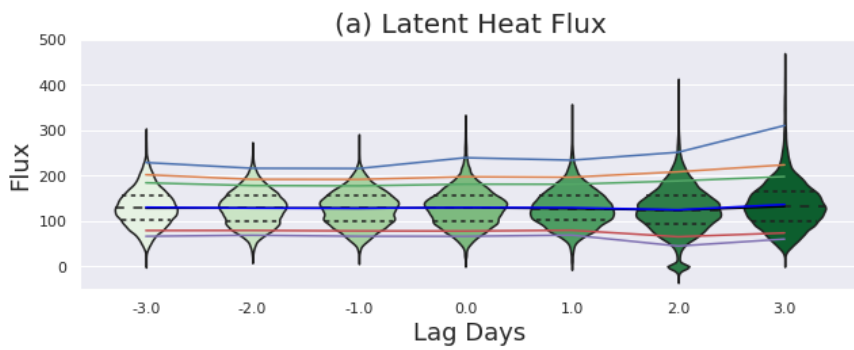
(a) Latent Heat Flux
Flux
Lag Days

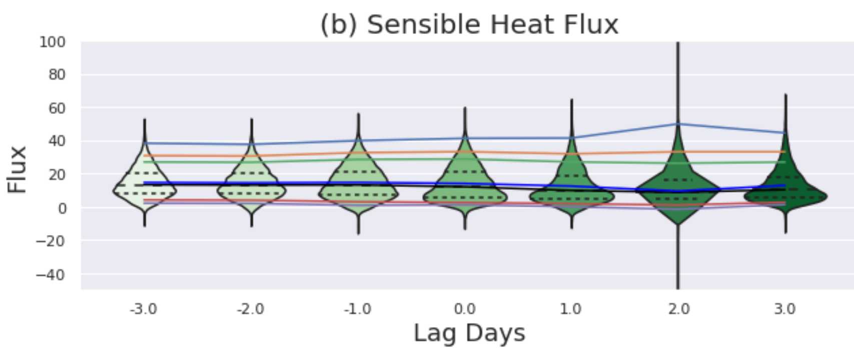
(b) Sensible Heat Flux
Flux
Lag Days

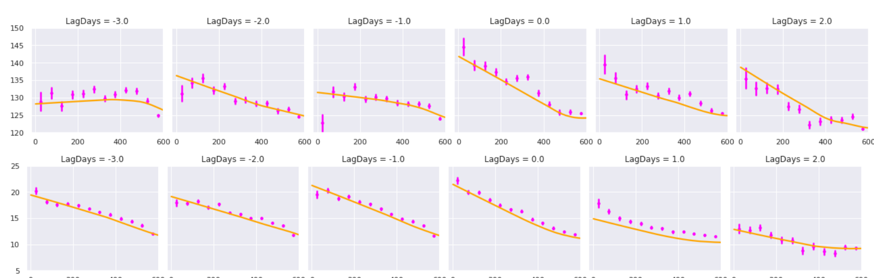
LagDays = -3.0
LagDays = -2.0
LagDays = -1.0
LagDays = 0.0
LagDays = 1.0
LagDays = 2.0

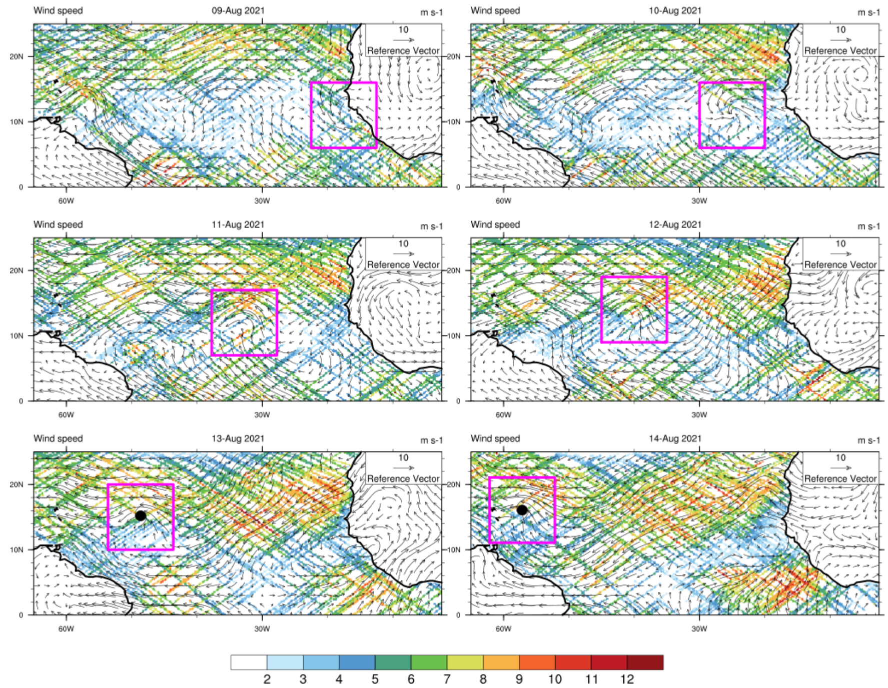
Wind speed
09-Aug 2021
10-Aug 2021
11-Aug 2021
12-Aug 2021
13-Aug 2021
14-Aug 2021
m s-1
10
Reference Vector
20N
10N
0
60W
30W
2
3
4
5
6
7
8
9
10
11
12

Surface Winds and Enthalpy Fluxes During Tropical Cyclone Formation From Easterly Waves: A CYGNSS view

Anantha Aiyyer[1] and Carl Schreck[2]

[1]Department of Marine Earth and Atmospheric Sciences, North Carolina State University, Raleigh, NC USA.

[2]Cooperative Institute for Satellite Earth System Studies (CISESS), North Carolina State University, Asheville, NC

Key Points:

- CYGNSS winds clearly depict the climatological easterly wave stormtrack
- A precursor vortex (proto-vortex) is seen in surface wind fields as early as 3 days prior to the tropical cyclone formation.
- An inward increase of surface enthalpy fluxes within the proto-vortex is seen prior to the tropical cyclone formation.

Corresponding author: Anantha Aiyyer, `aaiyyer@ncsu.edu`

Abstract

We examined the Cyclone Global Navigation Satellite System (CYGNSS) retrievals of surface winds and enthalpy fluxes in African easterly waves that led to the formation of 31 Atlantic tropical cyclones from 2018–2021. Lag composites show a cyclonic proto-vortex as early as 3 days prior to tropical cyclogenesis. The distribution of enthalpy fluxes within the proto-vortex does not vary substantially prior to cyclogenesis, but subsequently, there is an increase in the upper extreme values. A negative radial gradient of enthalpy fluxes becomes apparent as early as 2 days before cyclogenesis. These results—based on a novel data blending satellite retrievals and global reanalysis—are consistent with recent studies that have found that tropical cyclone spin-up is associated with a shift of peak convection towards the vortex-core and a radially inward increase of enthalpy fluxes. They provide additional evidence for the importance of surface enthalpy fluxes and their radial structure for tropical cyclogenesis.

Plain Language Summary

We used data derived from the recently launched Cyclone Global Navigation Satellite System (CYGNSS) to examine the surface winds and heat fluxes during the transition of easterly waves to tropical cyclones in the Atlantic. The CYGNSS winds show a proto-vortex in place 3 days before the formation of the tropical cyclone. The heat fluxes from the ocean to the air—which fuel the tropical cyclone—are enhanced near the core of the developing vortex as compared to the outer regions. This is consistent with past theoretical and observational studies, and likely contributes to the development of a deep moist column of air that typically precedes tropical cyclogenesis. The novelty of this paper lies in the use of a new data set and emphasis on the period leading up to tropical cyclogenesis from easterly waves.

1 Introduction

Tropical cyclogenesis typically proceeds from organized precipitating convection within deep saturated air columns (e.g., Emanuel, 2018). In principle, tropical cyclones can emerge spontaneously and no special precursors are necessary (e.g, Hakim, 2011; Wing et al., 2020). That notwithstanding, in our current climate, tropical cyclones are observed to form from mesoscale convection that is typically embedded within a preexisting larger-scale disturbance (Schreck et al., 2012). What elements of spontaneous self-aggregation are active within preexisting synoptic-scale disturbances in a fully varying background flow? That question remains a subject of active research. Documenting, in detail, the characteristics of tropical cyclone precursors observed in nature is important in that regard. Here we examine some surface characteristics of African easterly waves (AEWs) during the time when they were developing into tropical cyclones.

McBride and Zehr (1981) found that developing easterly waves tended to have stronger low-level relative vorticity and weaker environmental vertical wind shear compared to non-developing ones. Subsequent studies have expanded the parameter space to include thermal structure, the vigor of precipitating convection, environmental moisture and convective cloud fraction (e.g., Hopsch et al., 2010; Komaromi, 2013; Davis et al., 2014). Leppert et al. (2013) and Zawislak and Zipser (2014) suggested that, while the intensity of convection is not a discriminator of tropical cyclogenesis, developing easterly waves were associated with a greater fractional area of intense convection as compared to non-developing ones. Fritz et al. (2016) and Zawislak (2020) reported enhanced intensity and areal coverage of precipitation prior to tropical cyclogenesis. On the other hand, Wang (2018) reported large variability in the intensity, frequency, and area of deep convection during tropical cyclogenesis. Interestingly, she found one consistent feature—during tropical cyclogenesis, intense convection tended to cluster within the center of the incipient vortex while outside this core region, it remains unchanged or might even weaken.

The aforementioned studies have utilized a variety of data (e.g., global reanalysis, dropsondes, satellite-derived cloud properties, and precipitation), but have tended to focus on tropospheric parameters. Scant attention has been devoted to the role of surface enthalpy fluxes within the precursor waves prior to tropical cyclogenesis. Indeed, Murthy and Boos (2018) noted that, in general, the role of surface enthalpy flux during the spin-up of a tropical cyclone is still being debated. On the other hand, once a tropical cyclone has formed, surface enthalpy fluxes have been shown to be critical for its subsequent intensification (Emanuel, 2018). One particular instability mechanism —wind-induced surface heat exchange (WISHE)—relies on positive feedback between surface winds and enthalpy fluxes and is activated once a mesoscale saturated column of air is established (Zhang & Emanuel, 2016). Murthy and Boos (2018) attempted to address the role of surface enthalpy fluxes during the initial spin-up of a tropical cyclone (i.e., the tropical depression stage) using idealized simulations. One of their key findings was that a negative radial gradient of surface enthalpy flux is necessary for the genesis of a tropical cyclone from a precursor vortex.

The majority of past investigations of surface fluxes in tropical cyclones have relied on numerical simulations. Relatively few have been able to exploit direct flux observations (e.g., Cione et al., 2000; Bell et al., 2012). As these measurements are typically sourced from buoys, field campaigns, and coastal observing stations, they lack the spatial and temporal coverage that is needed for detailed diagnostics. Some studies have used surface fluxes derived from remotely sensed data (e.g., Liu et al., 2011); but they have tended to focus on the intensification of tropical cyclones. To our knowledge, no prior study dealing with surface winds and enthalpy fluxes in AEWs undergoing tropical cyclogenesis has been reported in the published literature.

In this paper, we document the composite structure of surface winds and enthalpy (latent and sensible heat) fluxes associated with developing AEWs. We used data from the recently launched NASA Cyclone Global Navigation Satellite System (CYGNSS) mission which consists of a constellation of low-earth orbiting satellites (Ruf et al., 2016).

2 Data

We used the following data covering July–October 2018-2021.

- CYGNSS surface winds – Level 3 Science Data Record (SDR), version 3.1 (Ruf et al., 2016). We use the fully developed seas (FDS) wind speeds that are provided hourly on a $0.2{\times}0.2^o$ grid within about 40^o north and south of the equator. We averaged the hourly data to create daily mean fields prior to subsequent processing.
- 10m winds and sea level pressure from the ERA5 reanalysis (Hersbach et al., 2020).
- CYGNSS surface latent and sensible heat flux (Level 2 SDR 2.0) that are based on the SDR 3.1 wind retrievals and ERA5 thermodynamic fields. Some additional information regarding the CYGNSS data, including an example of CYGNSS winds associated with a typical AEW, is included in the supporting information.
- Following Russell et al. (2017), to ascertain which Atlantic tropical cyclones developed from AEWs, we use the storm reports prepared by the US National hurricane center (NHC). We only considered those tropical cyclones that were specifically attributed to a wave that emerged from the west coast of Africa

3 Results

3.1 Climatalogical Surface Winds Over The Tropical Atlantic

We first show that the CYGNSS winds are capable of depicting the climatology mean as well as the synoptic variability of surface winds over the tropical Atlantic. The mean and variance of the daily averaged CYGNSS (FDS) winds for July–October 2018-2021, along with the climatological (1980–2018) mean sea level pressure, is presented in Figure 1. The CYGNSS winds clearly show the presence of the Atlantic subtropical anticyclone, consistent with the spatial structure seen in the ERA5 sea level pressure contours. The low-level jet over the Caribbean can also be seen. This jet has been suggested to be important for the amplification of easterly waves crossing into the eastern Pacific (Molinari et al., 1997). The mean winds are generally weaker within the main development region MDR (marked by the rectangle). The low-level westerly monsoon flow can be deduced from the enhanced wind speeds over the near-equatorial eastern Atlantic. On the other hand, the African easterly jet (AEJ) which, on average is located around 12^{o}N and peaks in the mid-troposphere, does not appear to extend down to the surface as noted from the lack of any wind maximum off the coast of west Africa.

Figure 1b shows a zonally oriented region of enhanced wind variance within the MDR—between 5^{o}N–15^{o}N, and from the west coast of Africa to 60^{o}W. This enhanced variance occurs where the mean wind is weak (Fig. 1a). The atmospheric variability in the off-equatorial tropical Atlantic is dominated by synoptic-scale waves during July–October (e.g., Mekonnen et al., 2006). Thus, we infer that this region of enhanced variance depicts the surface signal of the AEW stormtrack in the CYGNSS winds. Albeit episodic, tropical cyclones will also contribute to the daily wind variance as discussed by Schreck et al. (2012). Just off the west coast of Africa, around 20^{o}N, a small band of enhanced variance can be noted. We associate this with the surface reflection of the northern AEW stormtrack that exists poleward of the African easterly jet (e.g., Thorncroft & Pytharoulis, 2001; Diaz & Aiyyer, 2013). The northern AEW stormtrack appears to merge with the southern AEW stormtrack between 20^{o}W-30^{o}W. The aforementioned features seen in the variance of CYGNSS winds are consistent with AEW stormtracks seen in 850-hPa synoptic-scale eddy kinetic energy derived from global reanalysis fields (e.g. Russell & Aiyyer, 2020). One additional feature is notable in Figure 1 – over the Caribbean, the enhanced surface wind variance is shifted west of the peak surface winds. This downstream shift of eddy activity relative to the low-level Caribbean jet is consistent with the notion that easterly waves may form or amplify owing to the instability of the background flow in this region (Molinari et al., 1997).

3.2 Composite Wind Structures During Tropical Cyclogenesis

We now consider the evolution of surface winds during the time of tropical cyclogenesis from AEWs. A total of 31 tropical cyclones were identified by the NHC as originating from AEWs within the MDR during the study period. The genesis locations of these storms are shown in Figure S2. To document the surface wind evolution, we calculated storm-relative composite means as follows. We shifted the data grids such that all storms shown in Figure S2 are co-located at a reference point (10^oN; 40^oW) on the day of tropical cyclogenesis (Day-0). For lag-composites, we moved the date of the composite forward and backward while retaining the same spatial shift. Although there may be considerable storm-to-storm variability, such compositing techniques elucidate the features that are most likely to occur in a synoptic phenomenon (Wang, 2018).

The composite CYGNSS (FDS) speeds and 10-m ERA5 velocity vectors are shown in the left panel of Figure 2. The right panel shows the same fields but as anomalies relative to a background mean that was calculated by averaging over 13 days centered on Day-0 for each storm in the composite. For a vector in the composite field to be deemed statistically significant (shown by bold arrows), either its zonal or the meridional component must be significant. The statistical significance of each wind component was evaluated by comparing it against 1000 composites, each created by randomly drawing 31 dates over July–October, 2018–2021. A two-tailed significance was evaluated at the 95% confidence level with the null hypothesis being that the composite average could have resulted from a random draw.

Figure 2 shows that there is a close correspondence between the structure of the CYGNSS retrievals and ERA5 near-surface winds. An incipient surface vortex (marked by the filled square) is beginning to appear on Day-4, and becomes more coherent on Day-3. The proto-vortex associated with the composite AEW moves westward and continues to amplify. In part, this increased coherence is expected simply as a result of the compositing method as we get closer to Day-0. Nevertheless, it shows that a surface-based vortex with closed circulation is in place 3–4 days prior to the tropical depression stage.

This is consistent with the notion of a proto-vortex embedded within a synoptic scale wave pouch that is often visualized in a wave-following reference frame (e.g., Dunkerton et al., 2009). Interestingly, the composite surface vortex is visible here even in the earth-relative frame.

The leading and trailing anticyclonic anomalies straddling the main vortex can also be seen, particularly in the anomaly fields. Despite the minimal data filtering employed here–in the form of removing the 13-day mean flow—these features clearly highlight the AEW wavepacket in the surface wind fields, consistent with those seen in 2-10 day filtered fields at 850 hPa (e.g., Diaz & Aiyyer, 2013).

4 Surface Enthalpy fluxes within AEWs

Figure 3 illustrates the distribution of latent and sensible heat fluxes as a function of time relative to tropical cyclogenesis using data from all 31 AEWs considered in this study. For each day, we extracted all available flux values for each wave within a radial distance of 700 km from the center of the tracked composite vortex (see fig. 2). The extent of this region is roughly half the canonical AEW wavelength (e.g., Diaz & Aiyyer, 2015) and represents the cyclonic circulation of the wave. The overall qualitative interpretation of our subsequent findings is not sensitive to the dimension of this bounding region as long as it encompasses the bulk of the AEW trough.

Figure 3a shows an expansion of the upper extremes of the Latent heat flux distribution over time. The 99^{th} and 95^{th} percentile values increase by 36% and 11%, respectively, from Day-3 to Day +3. These increases occur subsequent to tropical cyclogenesis. On the other hand, the mean and median values barely change. They increase only by 5% and 3% respectively. On average, the sensible heat fluxes (3b) are about 10 times smaller than the latent heat fluxes. From Day-3 to Day+3, the 99^{th} and 95^{th} percentile values of the sensible heat fluxes increase by 16% and 8%, respectively. Intriguingly, the mean and median of these fluxes decrease by roughly 10% and 22% respectively. From Fig. 3, it can be noted that this decrease occurs mostly after the tropical depression has formed.

The increase in the upper extremes of both sensible and latent fluxes is unsurprising since peak surface wind speeds increase after the genesis of the tropical cyclone. However, the key result from Fig. 3 is that the mean surface enthalpy fluxes do not change substantially during the 3 days prior to tropical cyclogenesis. Rather, the bulk of the change occurs after the formation of the tropical depression, and likely reflects its subsequent intensification into a tropical cyclone. Thus, the intensity of surface enthalpy fluxes within the AEW may not be a particularly good predictor of imminent cyclogenesis. On the other hand, the robust expansion of the upper extremes ($> 90^{th}$ percentile) of their distributions suggests that localized sharp increases in surface fluxes accompany tropical cyclogenesis and further intensification.

We now examine whether there is a discernible change in the radial structure of the surface enthalpy fluxes in the developing vortex within the AEW. For each day relative to cyclogenesis, we binned all available fluxes (for all 31 AEWs) based on the distance from the center of the vortex tracked in Fig. 2. We show the results for 50 km bin width in Fig. 4. The interpretation was qualitatively similar when we used other reasonable values for the bin width ranging from 20–70 km. Fig. 4 illustrates the result of the binning in two ways, representing simple measures of azimuthally averaged fluxes as a function of distance (radius) from the vortex center. The bars show the mean flux and its 95% confidence interval for each bin, and the orange line shows the non-parametric locally weighted scatterplot smoothing (LOWESS) regression curve. The LOWESS curve was calculated using all data points prior to binning them.

Two key observations from Fig. 4 can be made. First, up to three days before the formation of the tropical depression, the sensible heat flux is nearly radially uniform. A similar picture was seen on Day-4 and earlier (not shown). On the other hand, there is already a clear inward increase (i.e., negative radial gradient) in the sensible heat flux by Day-3. Second, closer to cyclogenesis (Day-2 and Day-1), a negative radial gradient of latent heat fluxes is also evident. As expected, due to the way the flux data are aggregated based on the composite vortex center, the strength of this negative radial gradient is most striking on the reference day (Day 0). But despite the differences in the subsequent tracks and motion of the developing tropical cyclone, this negative radial gradient is also present on Day+1 and Day+2. Wang (2018) showed that, during the time leading up to cyclogenesis, intense convection appears to move towards the center of the proto-vortex. She also found that, in the outer parts of the proto-vortex, the intensity of convection is unchanged or even reduced. This concentration of convection is likely supported by increasing values of surface enthalpy fluxes in the core of the vortex as seen in Fig. 4, and is consistent with the modeling work of Murthy and Boos (2018).

Some features seen in Fig. 4 need additional scrutiny. That the negative radial gradient is seen earlier for the sensible heat flux is an intriguing result. It also appears that the area-mean sensible heat flux is diminished by Day+2 as compared to earlier days. The reason for these observations is unclear from our analysis and calls for high-resolution numerical simulations with interactive air-sea coupling.

5 Discussion

The establishment of a saturated column of air is a critical step toward cyclogenesis because evaporation-driven downdrafts are reduced and the environment becomes conducive for deep convection, setting the stage for the WISHE process (Emanuel, 2018). Molinari et al. (2004) described two stages of hurricane development: A pre-WISHE stage, wherein the radial profile of near-surface equivalent potential temperature (θ_e), a measure of moist entropy, was nearly radially uniform; and a WISHE stage with a single dominant surface vortex with a moist core and marked inward increase (i.e., a negative gradient) of θ_e, consistent with the steady-state model of Smith (2003). As noted by Murthy and Boos (2018), axisymmetric models of tropical cyclogenesis require a negative gradient of column relative humidity (e.g., Emanuel, 1997; Frisius, 2006; Smith, 2003). On the basis of their idealized numerical simulations, Murthy and Boos (2018) argued that an inward increase in surface enthalpy fluxes is one possible pathway to get a persistent saturated core within a precursor vortex. This motivated us to examine the evolution of surface latent heat fluxes within AEWs leading to tropical cyclogenesis. We summarize our results for two periods:

- *Prior to tropical depression formation*: The CYGNSS-derived surface latent heat fluxes within the composite precursor vortex increase only modestly during the period leading to the depression stage of tropical cyclogenesis (Fig. 3). Since we did not compare developing and non-developing AEWs, we cannot ascertain whether these developing waves were associated with some minimal threshold of surface fluxes that would maintain the precursor vortex or AEW. However, it appears - at least from the aggregate view – that a rapid increase in the average surface latent heat fluxes is not a necessary step for cyclogenesis; rather it occurs after the depression has formed. Surface enthalpy fluxes are nearly radially uniform up to 3 days prior to the formation of the composite tropical depression. Following Molinari et al. (2004), this would correspond to the pre-WISHE stage of tropical cyclone development.

Interestingly, during the two days leading to cyclogenesis, a clear negative radial gradient of surface enthalpy fluxes is established. This suggests a spatial reorganization of surface fluxes – and by extension, intense moist convection – that favors a shift towards the core of the developing vortex. This is consistent with the findings of Wang (2018). This radially inward increase of surface enthalpy flux likely sets the stage for tropical cyclogenesis, and is consistent with the model simulations of tropical cyclone spin-up from a proto-vortex described by Murthy and Boos (2018).

- *Post tropical depression formation*: There is a widening of the surface enthalpy flux distribution towards higher values within the developing vortex (Fig. 3). The upper extreme of the latent heat flux distribution increases substantially a day after the depression has formed. As noted by (Wang, 2018), the migration of convection towards the core of the developing vortex is the key feature of tropical cyclogenesis. Importantly, and related to the migration of deep convection, a clear inward increase of surface enthalpy fluxes becomes a persistent feature (Fig. 4). Following the arguments of Murthy and Boos (2018) and Molinari et al. (2004), the rapid increase in the latent heat fluxes and the presence of a negative radial gradient of the fluxes in the intensifying vortex indicates that the WISHE mechanism is now fully active.

There are a few caveats to consider in relation to the data and method used here. The surface enthalpy fluxes are dependent on the fidelity of ERA5's surface thermodynamic fields and incur the attendant errors and biases. Additionally, we did not track the precursor AEWs, and instead used lag-composites to visualize the evolution of the fields. An alternative method would be to track the waves, which introduces other uncertainties stemming from multiple vorticity centers, splits, and mergers. We favor our current method for the ease of reproducibility. The coherence of the composite fields at different times (Fig. 2) gives us confidence that the wave-to-wave variability in tracks does not alter our conclusions.

6 Conclusions

The CYGNSS retrievals capture the mean spatial structure of surface winds over the tropical Atlantic and the synoptic-scale AEW stormtrack. Lag-composites of CYGNSS and ERA5 data show a clear signal of an AEW wavepacket and an attendant, low-level cyclonic vortex as early as 3 days prior to the tropical cyclogenesis. The distribution of surface enthalpy fluxes within the proto-vortex does not change substantially prior to the tropical depression formation. Subsequently, the distribution widens, indicating amplified fluxes. Up to 3 days before the depression stage, the surface latent fluxes within the precursor vortex are nearly radially uniform. Subsequently, from Day-2 onward, a clear negative radial gradient of both latent and sensible heat fluxes is established. These results are consistent with a recent modeling study that found that an inward increase of surface enthalpy fluxes is important for the spin-up of tropical cyclones (Murthy & Boos, 2018).

7 Open Research

The CYGNSS wind and surface enthalpy fluxes are available at, respectively, `https://doi.org/10.5067/CYGNS-L3X31` and `https://doi.org/10.5067/CYGNS-L2H20`. The ERA5 fields are available at `https://cds.climate.copernicus.eu`. The IBTRACS database of tropical cyclone tracks is archived at `https://doi.org/10.25921/82ty-9e16`.

Acknowledgments

We are grateful to Juan Crespo for the CYGNSS heat fluxes. This work was supported by NASA through awards NNX17AH61G and 80NSSC22K0610.

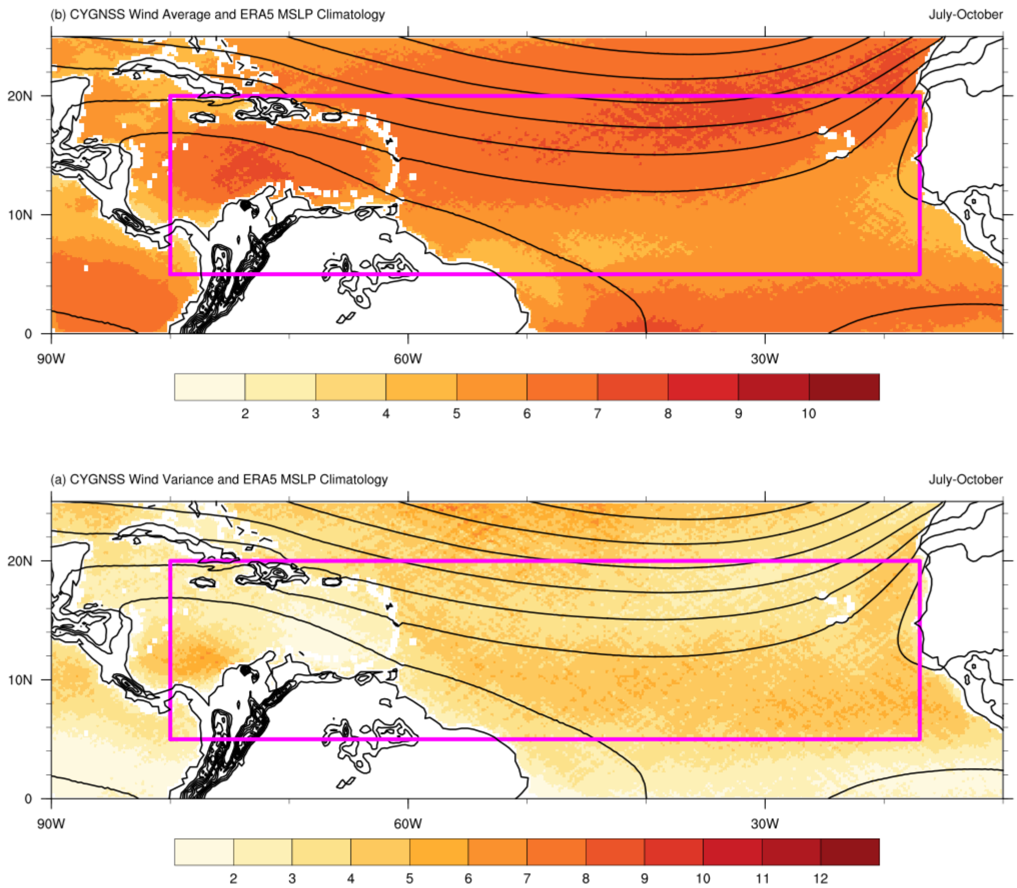

Figure 1. Shaded fields showing (a) Variance (m^2s^{-2}) ; and (b) mean (ms^{-1}) of daily averaged CYGNSS FDS wind speed over July-October 2018–2021. The contours on both panels show the long-term (1980-2018) climatology of mean sea level pressure from ERA5. The magenta rectangle marks the main development region considered in this paper.

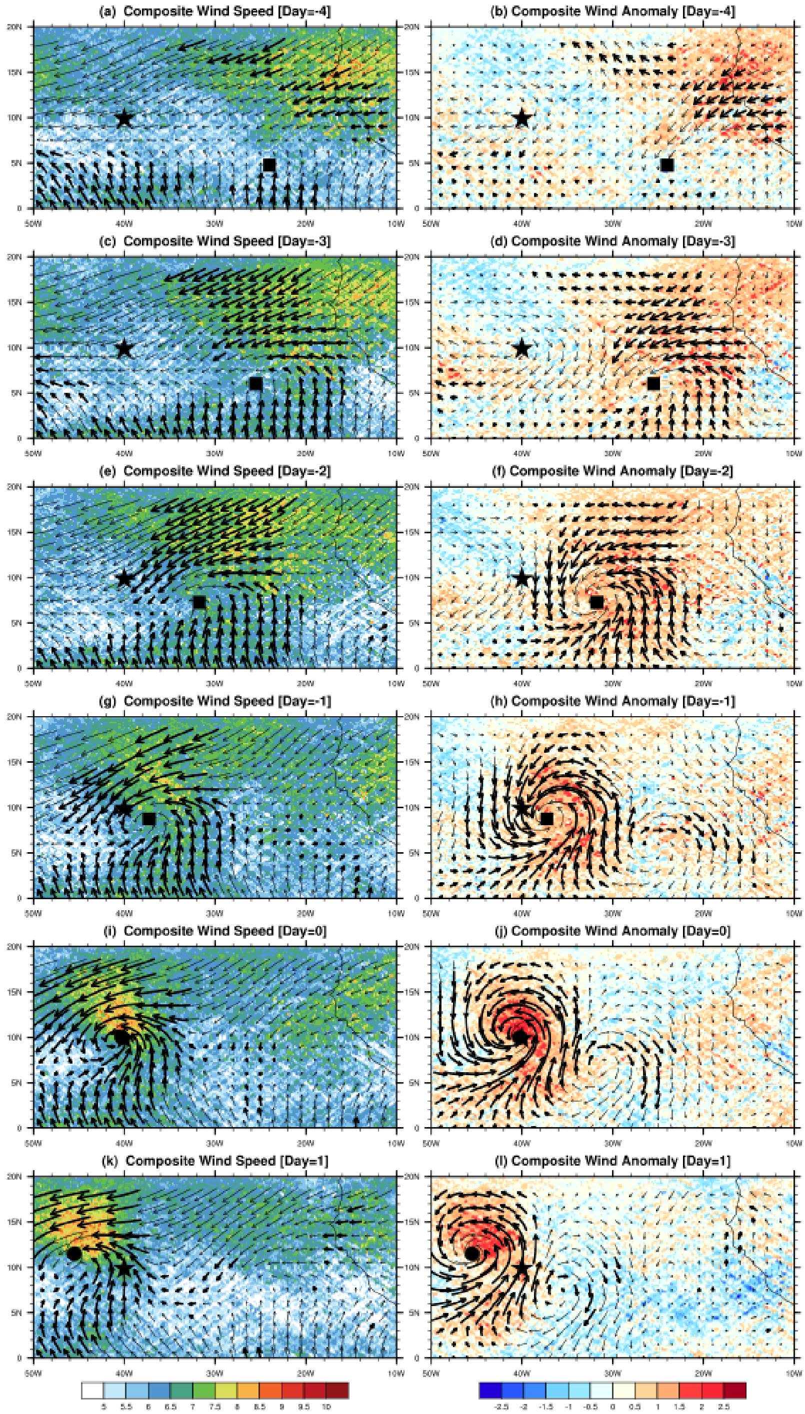

Figure 2. Storm centered lag composite mean (left panels) and anomalies (Right panels) of CYGNSS FDS wind speeds (shaded) and ERA5 10m wind vectors. The star symbol marks the center of the composite storm at the first recorded depression stage corresponding to Day 0. The black square shows the incipient vortex within the composite AEW, and the hurricane symbol marks the location of the composite tropical storm after it has formed.

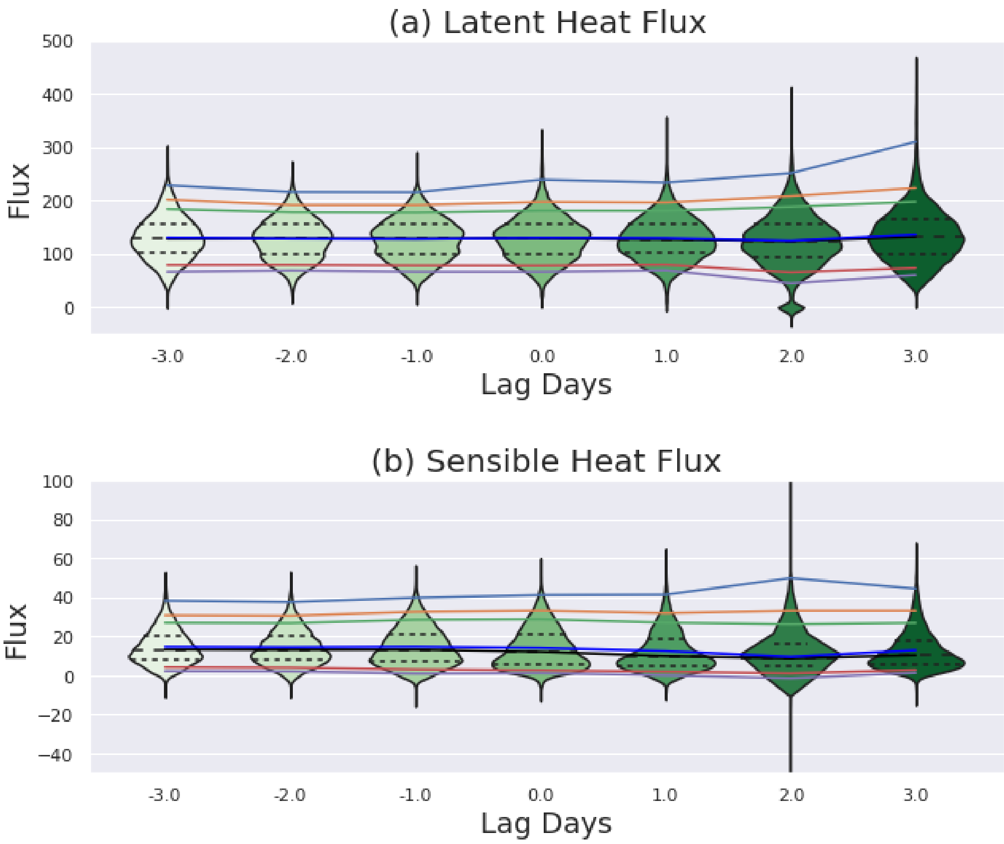

Figure 3. Distribution of (a) latent; and (b) sensible heat fluxes (Wm^{-2}) within a radial distance of 700 km from the composite vortex center (see Fig. 2) at different days relative to tropical cyclogenesis. The blue solid line marks the mean of the distributions. The rest of the solid lines depict, from bottom to top, the following percentiles of the distribution: P_5, P_{10},P_{50} (median), P_{90}, P_{95}, and P_{99}.

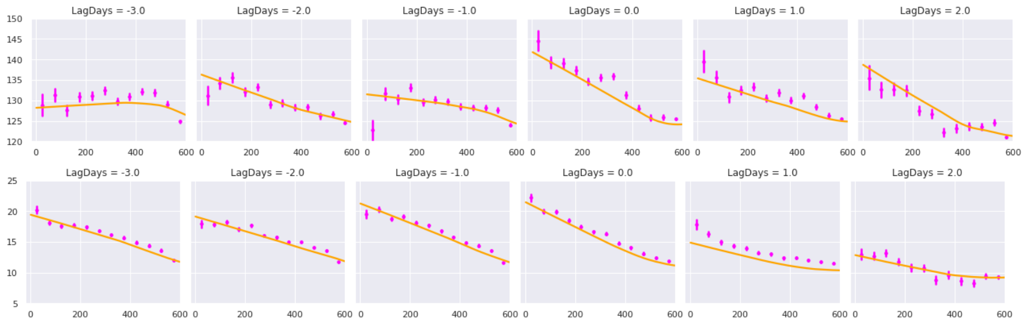

Figure 4. Latent (top panels) and sensible (bottom panels) heat fluxes ($\mathrm{Wm^{-2}}$) as a function of distance (km) from the vortex center at different days relative to tropical cyclogenesis. The fluxes were binned at 50 km radial increments. The bars show the mean flux for each bin and its 95% confidence interval. The orange line shows the non parametric LOWESS regression fit that was calculated using un-binned data

References

Bell, M. M., Montgomery, M. T., & Emanuel, K. A. (2012, November). Air-Sea Enthalpy and Momentum Exchange at Major Hurricane Wind Speeds Observed during CBLAST. *Journal of Atmospheric Sciences*, *69*(11), 3197-3222. doi: 10.1175/JAS-D-11-0276.1

Cione, J. J., Black, P. G., & Houston, S. H. (2000, May). Surface Observations in the Hurricane Environment. *Monthly Weather Review*, *128*(5), 1550.

Davis, C. A., Ahijevych, D. A., Haggerty, J. A., & Mahoney, M. J. (2014, May). Observations of Temperature in the Upper Troposphere and Lower Stratosphere of Tropical Weather Disturbances. *Journal of Atmospheric Sciences*, *71*(5), 1593-1608. doi: 10.1175/JAS-D-13-0278.1

Diaz, M., & Aiyyer, A. (2015, May). Absolute and Convective Instability of the African Easterly Jet. *J. Atmos. Sci.*, *72*(5), 1805-1826. doi: 10.1175/JAS-D-14-0128.1

Diaz, M. L., & Aiyyer, A. (2013). Energy Dispersion in African Easterly Waves. *J. Atmos. Sci.*, *70*, 130-145. doi: 10.1175/JAS-D-12-019.1

Dunkerton, T. J., Montgomery, M. T., & Wang, Z. (2009, August). Tropical cyclogenesis in a tropical wave critical layer: easterly waves. *Atm. Chem. & Phys.*, *9*, 5587-5646.

Emanuel, K. (1997, April). Some Aspects of Hurricane Inner-Core Dynamics and Energetics. *Journal of Atmospheric Sciences*, *54*(8), 1014-1026.

Emanuel, K. (2018). 100 Years of Progress in Tropical Cyclone Research. In *Meteorological monographs, vol. 59, pp. 15.1-15.68* (Vol. 59, p. 15.1-15.68). doi: 10.1175/AMSMONOGRAPHS-D-18-0016.1

Frisius, T. (2006, October). Surface-flux-induced tropical cyclogenesis within an axisymmetric atmospheric balanced model. *Quarterly Journal of the Royal Meteorological Society*, *132*(621), 2603-2623. doi: 10.1256/qj.06.03

Fritz, C., Wang, Z., Nesbitt, S. W., & Dunkerton, T. J. (2016, January). Vertical structure and contribution of different types of precipitation during Atlantic tropical cyclone formation as revealed by TRMM PR. *Geophys. Res. Letts.*, *43*(2), 894-901. doi: 10.1002/2015GL067122

Hakim, G. J. (2011, June). The Mean State of Axisymmetric Hurricanes in Statistical Equilibrium. *J. Atmos. Sci.*, *68*(6), 1364-1376. doi: 10.1175/2010JAS3644

.1

Hersbach, H., Bell, B., Berrisford, P., Hirahara, S., Horányi, A., Muñoz-Sabater, J., ... Thépaut, J.-N. (2020). The era5 global reanalysis. *Quarterly Journal of the Royal Meteorological Society*, *146*(730), 1999-2049. doi: https://doi.org/10.1002/qj.3803

Hopsch, S. B., Thorncroft, C. D., & Tyle, K. R. (2010, April). Analysis of African Easterly Wave Structures and Their Role in Influencing Tropical Cyclogenesis. *Monthly Weather Review*, *138*(4), 1399-1419. doi: 10.1175/2009MWR2760.1

Komaromi, W. A. (2013, February). An Investigation of Composite Dropsonde Profiles for Developing and Nondeveloping Tropical Waves during the 2010 PREDICT Field Campaign. *Journal of Atmospheric Sciences*, *70*(2), 542-558. doi: 10.1175/JAS-D-12-052.1

Leppert, I., Kenneth D., Cecil, D. J., & Petersen, W. A. (2013, August). Relation between Tropical Easterly Waves, Convection, and Tropical Cyclogenesis: A Lagrangian Perspective. *Monthly Weather Review*, *141*(8), 2649-2668. doi: 10.1175/MWR-D-12-00217.1

Liu, J., Curry, J. A., Clayson, C. A., & Bourassa, M. A. (2011, September). High-Resolution Satellite Surface Latent Heat Fluxes in North Atlantic Hurricanes. *Monthly Weather Review*, *139*(9), 2735-2747. doi: 10.1175/2011MWR3548.1

McBride, J. L., & Zehr, R. (1981, June). Observational analysis of tropical cyclone formation. Part II: comparison of non-developing versus developing systems. *J. Atmos. Sci.*, *38*, 1132-1151.

Mekonnen, A., Thorncroft, C. D., & Aiyyer, A. R. (2006). Analysis of Convection and Its Association with African Easterly Waves. *J. Climate*, *19*, 5405-5421. doi: 10.1175/JCLI3920.1

Molinari, J., Knight, D., Dickinson, M., Vollaro, D., & Skubis, S. (1997). Potential vorticity, easterly waves, and eastern pacific tropical cyclogenesis. *Mon. Wea. Rev.*, *125*, 2699-2708.

Molinari, J., Vollaro, D., & Corbosiero, K. L. (2004, November). Tropical Cyclone Formation in a Sheared Environment: A Case Study. *Journal of Atmospheric Sciences*, *61*(21), 2493-2509. doi: 10.1175/JAS3291.1

Murthy, V. S., & Boos, W. R. (2018, June). Role of Surface Enthalpy Fluxes in Idealized Simulations of Tropical Depression Spinup. *Journal of Atmospheric Sci-*

ences, *75*(6), 1811-1831. doi: 10.1175/JAS-D-17-0119.1

Ruf, C. S., Atlas, R., Chang, P. S., Clarizia, M. P., Garrison, J. L., Gleason, S., ... Zavorotny, V. U. (2016, March). New Ocean Winds Satellite Mission to Probe Hurricanes and Tropical Convection. *Bulletin of the American Meteorological Society*, *97*(3), 385-395. doi: 10.1175/BAMS-D-14-00218.1

Russell, J., & Aiyyer, A. (2020, March). The Potential Vorticity Structure and Dynamics of African Easterly Waves. *J. Atmos. Sci.*, *77*(3), 871-890. doi: 10.1175/JAS-D-19-0019.1

Russell, J., Aiyyer, A., White, J. D., & Hannah, W. (2017, January). Revisiting the connection between African Easterly Waves and Atlantic tropical cyclogenesis. *Geophys. Res. Letts.*, *44*(1), 587-595. doi: 10.1002/2016GL071236

Schreck, I., Carl J., Molinari, J., & Aiyyer, A. (2012, Mar). A Global View of Equatorial Waves and Tropical Cyclogenesis. *Mon. Wea. Rev.*, *140*(3), 774-788. doi: 10.1175/MWR-D-11-00110.1

Smith, R. K. (2003, January). A simple model of the hurricane boundary layer. *Quarterly Journal of the Royal Meteorological Society*, *129*(589), 1007-1027. doi: 10.1256/qj.01.197

Thorncroft, C., & Pytharoulis, I. (2001). A dynamical approach to seasonal prediction of atlantic tropical cyclone activity. *Wea. Forecasting*, *16*, 725-734.

Wang, Z. (2018, May). What is the Key Feature of Convection Leading up to Tropical Cyclone Formation? *Journal of Atmospheric Sciences*, *75*(5), 1609-1629. doi: 10.1175/JAS-D-17-0131.1

Wing, A. A., Stauffer, C. L., Becker, T., Reed, K. A., Ahn, M.-S., Arnold, N. P., ... Zhao, M. (2020, September). Clouds and Convective Self-Aggregation in a Multimodel Ensemble of Radiative-Convective Equilibrium Simulations. *Journal of Advances in Modeling Earth Systems*, *12*(9), e02138. doi: 10.1029/2020MS002138

Zawislak, J. (2020, April). Global Survey of Precipitation Properties Observed during Tropical Cyclogenesis and Their Differences Compared to Nondeveloping Disturbances. *Mon. Wea. Rev.*, *148*(4), 1585-1606. doi: 10.1175/MWR-D-18-0407.1

Zawislak, J., & Zipser, E. J. (2014, December). A Multisatellite Investigation of the Convective Properties of Developing and Nondeveloping Tropical Disturbances. *Monthly Weather Review*, *142*(12), 4624-4645. doi: 10.1175/MWR-D-14-00028.1

Zhang, F., & Emanuel, K. (2016, May). On the Role of Surface Fluxes and WISHE in Tropical Cyclone Intensification. *Journal of Atmospheric Sciences*, *73*(5), 2011-2019. doi: 10.1175/JAS-D-16-0011.1